

# Helical liquids and Majorana bound states in quantum wires

Yuval Oreg,<sup>1</sup> Gil Refael,<sup>2</sup> and Felix von Oppen<sup>3</sup>

<sup>1</sup>*Department of Condensed Matter Physics, Weizmann Institute of Science, Rehovot, 76100, Israel*

<sup>2</sup>*Department of Physics, California Institute of Technology, Pasadena, California 91125, USA and*

<sup>3</sup>*Dahlem Center for Complex Quantum Systems and Fachbereich Physik, Freie Universität Berlin, 14195 Berlin, Germany*

We show that the combination of spin-orbit coupling with a Zeeman field or strong interactions may lead to the formation of a helical liquid in single-channel quantum wires. In a helical liquid, electrons with opposite velocities have opposite spin precessions. We argue that zero-energy Majorana bound states are formed in various situations when the wire is situated in proximity to a conventional  $s$ -wave superconductor. This occurs when the external magnetic field, the superconducting gap, or the chemical potential vary along the wire. We discuss experimental consequences of the formation of the helical liquid and the Majorana bound states.

States of matter that support Majorana fermions have received much attention in the context of quantum computation. A widely separated pair of Majorana bound states forms a nonlocal fermionic state which is immune to local sources of decoherence, thus providing a platform for fault-tolerant quantum memory. Moreover, since Majorana states realize a representation of the non-Abelian braid group, topological quantum information processing can, in principle, be effected by braiding operations [1]. A realization of such states where they can be readily moved around and manipulated is therefore highly desirable.

There are several suggestions for physical systems that support Majorana states, for particular ways to manipulate them, and for measuring their properties. These include fractional quantum Hall states at filling factor  $\nu = 5/2$  [2],  $p$ -wave superconductors [3], surfaces of three-dimensional topological insulators in proximity to a superconductor [4], and helical edge modes of two-dimensional topological insulators in proximity to a ferromagnet and a superconductor [5]. Recently, it was suggested that a semiconducting thin film sandwiched between an  $s$ -wave superconductor and a magnetic insulator [6] will host Majorana states associated with superconducting vortices. All these proposals, however, would be experimentally extremely challenging.

Realizing and manipulating Majorana fermions in wires may be decisively simpler. Here we show that quantum wires with strong spin-orbit coupling, such as InAs or InSb wires, and banded carbon nanotubes form a helical liquid, similar to the edges of a topological insulator. Consequently, these wires support Majorana states when they are in proximity to  $s$ -wave superconductors, and a magnetic field. Most importantly, we explain how they can be produced and manipulated by variations of a chemical potential, which could be simply produced by a set of micron-sized gates capacitatively coupled to the wire. Below we outline the key physical properties of Majorana states in quantum wires, their experimental signatures, and how Majorana-supporting wires could be extended into networks of Majorana fermions, enabling

quantum information processing.

Our analysis begins with writing the Hamiltonian for a spin-orbit coupled quantum wire. Without loss of generality, let us choose the wire to lie along the  $y$  direction, the spin-orbit interaction,  $u$ , to be along the  $z$  direction, and a magnetic field  $B$  to be along the  $x$  direction. In addition, the wire is in contact with a superconductor, with the proximity strength being  $\Delta$  (assumed to be real). The Hamiltonian is given by [4]

$$H = \int \Psi^\dagger(y) \mathcal{H} \Psi(y) dy; \quad \Psi^\dagger = \left( \psi_{\uparrow}^\dagger, \psi_{\downarrow}^\dagger, \psi_{\downarrow}, -\psi_{\uparrow} \right) \quad (1)$$

$$\mathcal{H} = [p^2/2m - \mu(y)] \tau_z + u(y)p \sigma_z \tau_z + B(y) \sigma_x + \Delta(y) \tau_x.$$

Here,  $\psi_{\uparrow,(\downarrow)}(y)$  is the annihilation operator of electrons with up (down) spin at position  $y$ . The Pauli matrices  $\sigma$  and  $\tau$  operate in spin and particle-hole space, respectively.  $\mu$  is the chemical potential.

In the absence of the Zeeman field and the superconducting proximity, the eigenstates of the Hamiltonian (1) will have an energy-momentum dispersion consisting of two shifted parabolas crossing at momentum  $p = 0$ . The Zeeman field  $B$  removes the level crossing and opens a gap at  $p = 0$ . We note that such a gap may also occur due to strong electron-electron interactions [7, 8], and therefore  $B$  should be generally construed as either a magnetic field perpendicular to the spin orbit coupling, or an interaction induced gap. The pairing  $\Delta$  will play two crucial roles: Opening a gap at the outer wings of the dispersion, where the Zeeman field is unimportant, and modifying the gap forming near  $p = 0$ . The former role eliminates the possibility of high-momentum gapless excitations, thus leaving only the chiral states near  $p = 0$  as low energy excitation. These states resemble the edge of a topological insulator [4, 8]. The latter role allows us to tune the topological phase transitions essential for the production of Majorana fermions. Note that another way for gapping out the large momentum excitations is by coupling our system to an antiferromagnet with periodicity comparable to  $2k_F$  of the wire. Interactions may also open a pairing  $\pm k_F$  gap for chemical potentials away from the Zeeman gap [9].

The emerging spectrum for constant  $\mu$ ,  $u$ ,  $\Delta$ , and  $B$ , is conveniently obtained by squaring the Hamiltonian twice. This straightforwardly yields the expression:

$$E_{\pm}^2 = B^2 + \Delta^2 + \xi_p^2 + (up)^2 \pm 2\sqrt{B^2\Delta^2 + B^2\xi_p^2 + (up)^2\xi_p^2} \quad (2)$$

where  $\xi_p = p^2/2m - \mu$ . Fig. 1 displays the spectrum for several values of  $B$ ,  $\Delta$ , and  $\mu$ . As these parameters vary (while  $B$  and  $\Delta$  remain nonzero), a gap closing and re-opening indicates a topological phase transition. Generically, we expect gaps appearing near  $p = 0$  and near the Fermi momenta corresponding to  $\xi_p \pm up = 0$ . We will denote these gaps as  $E_0$  and  $E_1$ , respectively.

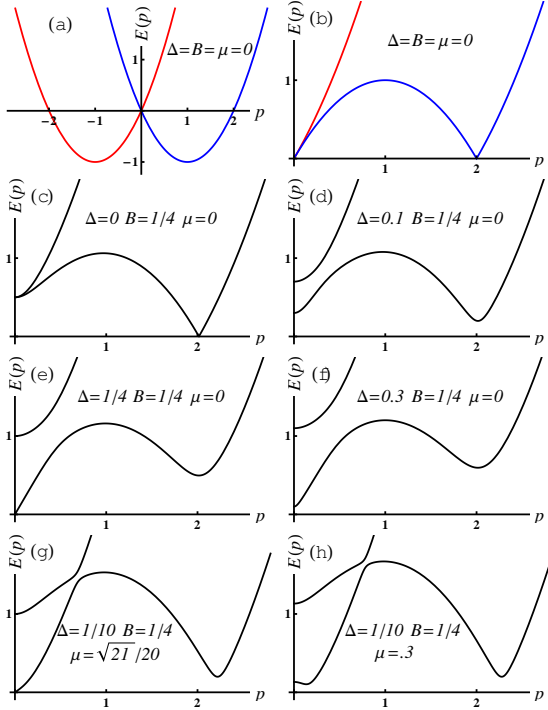


FIG. 1. (a) Single-particle spectrum for  $\mu = B = \Delta = 0$ . (The two colors denote the different spin components). The energy (momentum) scale is set by  $mu^2/2$  (by  $mu$ ), with  $u$  the spin-orbit coupling strength. (b) Excitation spectrum of adding or removing an electron for  $\mu = B = \Delta = 0$ . (c) Excitation spectrum for  $B = 1/4$ ,  $\Delta = \mu = 0$  where a spin gap opens near  $p = 0$ . (d)  $B = 2.5$ ,  $\Delta = 1/2$ ,  $\mu = 0$  with a superconducting gap in the wings and a spin gap near the origin. This situation is analogous to a  $p$ -wave superconductor. We refer to this phase as the "spin gap phase" (e)  $B = 1/4 = \Delta = 1/4$ ,  $\mu = 0$ . The gap near  $p = 0$  closes, the gap at finite  $p$  persists. At this critical point a quantum phase transition occurs. (f)  $B = 1/4$ ,  $\Delta = 0.3$ ,  $\mu = 0$ . All gaps in the excitation spectrum are controlled by  $\Delta$ . (g)  $B = 1/4$ ,  $\Delta = .1$ ,  $\mu = \sqrt{B^2 - \Delta^2} = \sqrt{21}/20$ . The gap at  $p = 0$  closes due to the shift in chemical potential. (h) A superconducting gap opens up in the entire spectrum due to the shift of the chemical potential above its critical value  $\Delta = 1/10$ ,  $B = 1/4$ ,  $\mu = 0.3$ .

As hinted above, it is the zero-momentum gap,  $E_0$ , which is crucial for our understanding of the emerging Majorana states. Examining  $E_-$  at  $p = 0$  we notice that

$$E_0 = E(p = 0) = |B - \sqrt{\Delta^2 + \mu^2}|. \quad (3)$$

For  $B^2 > \Delta^2 + \mu^2$ ,  $E_0$  is a spin gap due to the Zeeman field (or strong interaction), while for  $B^2 < \Delta^2 + \mu^2$  it is a superconducting gap, thus when  $B^2 = \Delta^2 + \mu^2$  a quantum phase transition occurs. At the same time the gap  $E_1$  near  $p^2 = 2\mu m$  is always a superconducting gap, as we require  $\Delta$  to always remain finite.

The phase transition evident in  $E_0$  allows the formation of *Majorana states*. Indeed, the dependence of  $E_0$  on  $B$ ,  $\Delta$ , and  $\mu$  enables us to construct zero-energy Majorana states in various ways. As in edge states of 2D topological insulators [4], a Majorana bound state will form when  $B$  changes in space and crosses  $\Delta$ , e.g. at  $y = 0$  (cf. Fig 2b), or when  $\Delta$  varies in space and crosses  $B$  (cf. Fig 2d).

Here we emphasize, however, a third possibility: varying the chemical potential,  $\mu$ . Let us assume that  $B > \Delta$  so that for  $\mu = 0$  we have a spin gap  $E_0$ . But when  $\mu > \sqrt{B^2 - \Delta^2}$ , the gap  $E_0$ , Eq. (3), is clearly superconducting. Thus, we can form a Majorana state by tuning  $\mu$  between these two values (cf. Fig 2c). We note that changes in  $\mu$  do not significantly influence the gap  $E_1$ , so that the electronic states near  $\pm k_F$  do not play a role.

The one-dimensional geometry allows for a simple demonstration of how to form Majorana states where their wave functions can be obtained essentially exactly. Let us consider these examples in a long ring with one conducting channel, in proximity to a superconductor and a Zeeman field, as illustrated in Fig. 2a. Since the relevant momenta are near  $p = 0$ , in the treatment below we use the Hamiltonian linearized in that region:

$$\mathcal{H} = up \sigma_z \tau_z - \mu(y) \tau_z + B(y) \sigma_x + \Delta(y) \tau_x \quad (4)$$

**Spatially varying  $B$ .** Assume  $\Delta > 0$  is constant,  $\mu = 0$ , and that  $B > \Delta$  for  $y > 0$  and  $B < \Delta$  for  $y < 0$  (Fig. 2b; note that the periodic boundary conditions require another point where  $B = \Delta$ ). Near the crossing point  $y = 0$ , we write  $B(y) = \Delta + by$ . Due to particle-hole symmetry, it is useful to square the Hamiltonian Eq. (4) to diagonalize it. In addition to the square of each term and the mixed  $B\Delta$  term, we obtain a term  $\{up\sigma_z\tau_z, B\sigma_x\} = i\sigma_y\tau_z u[p, B] = \sigma_y\tau_z ub$  which arises because  $B$  depends on space and does not anticommute with the spin-orbit coupling. Collecting all terms, we have

$$\mathcal{H}_b^2 = (up)^2 + B(y)^2 + \Delta^2 + ub\sigma_y\tau_z + 2\Delta B(y)\sigma_x\tau_x \quad (5)$$

Rotating  $\mathcal{H}_b^2$  by  $U_b^\dagger = 1/2(\tau_z - i\tau_x - i\sigma_x\tau_z + \sigma_x\tau_x)$ , we find that  $U_b \cdot \mathcal{H}_b^2 \cdot U_b^\dagger$  is diagonal with components  $(up)^2 + (\Delta \pm B)^2 \pm ub$ . The interesting modes are those

with a minus sign in the brackets,  $\Delta - B$ . They correspond to a simple harmonic oscillator Hamiltonian with ground-state wave function  $\varphi(y) = (b/(u\pi)^{1/4})e^{-by^2/(2u)}$  and energies  $E_n^2 = 2ub(n + 1/2) \pm ub$ ,  $n = 0, 1, 2, \dots$ . For  $b > 0$ , the minus sign yields a zero-energy state with Bogoliubov operator

$$\gamma_b^\dagger = \gamma_b = \frac{1}{\sqrt{2}}(\eta_1 - \eta_2) = \frac{1}{2}(\psi_\uparrow - i\psi_\downarrow + i\psi_\downarrow^\dagger + \psi_\uparrow^\dagger)$$

$$\eta_1 = 1/\sqrt{2}(\psi_\uparrow^\dagger + \psi_\uparrow); \quad \eta_2 = 1/(\sqrt{2}i)(\psi_\downarrow^\dagger - \psi_\downarrow). \quad (6)$$

The Majorana state at the second crossing point along the ring follows by  $b \rightarrow -b$ . Thus, this zero-energy state is  $E_0^+ = 0$  with Majorana operator  $-i/\sqrt{2}(\eta_1 + \eta_2)$ .

**Spatially varying  $\Delta$ .** For the case where  $\Delta$  depends on  $y$ , we assume  $\Delta(y) = B + dy$ ,  $\mu = 0$ , and a constant  $B$  (Fig.2c). The Hamiltonian here is similar to that in the  $y$ -dependent  $B$  case, if we exchange  $\tau$  and  $\sigma$  in Eqs. (4) and (5). Therefore, the Majorana states emerge in this case in exactly the same way as above, except with the diagonalizing matrices being  $U_d^\dagger = U_b^\dagger(\tau \leftrightarrow \sigma)$ , and with  $b$  and  $\Delta$  exchanged with  $d$  and  $B$  respectively in the resulting wave function. This yields (for positive  $d$ )  $\gamma_d = \gamma_d^\dagger = (\eta_1 - \eta_2)/\sqrt{2}$ .

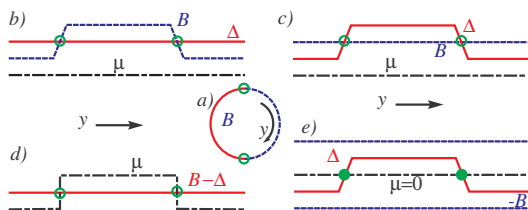


FIG. 2. (a) Wire in a ring geometry. Both halves have constant parameters and are joined by short junctions with a linearly varying parameter. Majorana states (marked by circles) are formed at the junctions. (b) Majorana state in the sector  $p = 0$  when  $B$  varies. The gap in the finite- $p$  sector remains finite in the entire wire. (c) Majorana state in the sector  $p = 0$  when  $\Delta$  varies. (d) Majorana state in the sector  $p = 0$  when  $\mu$  varies. (e) “ $p$ -wave” Majorana state when  $\Delta$  changes sign. The sector  $p = 0$  remains gapped in the entire wire. Each crossing with  $\Delta = 0$  hosts two Majorana states.

**Spatially varying  $\mu$ .** If  $B > \Delta$  in the entire wire, then at the interface between spin-gap regions with  $\mu^2 < B^2 - \Delta^2$  and pairing gap regions with  $|\mu|^2 > B^2 - \Delta^2$ , a Majorana state will also form (Fig.2d). In this case, we assume that  $\mu$  jumps abruptly at  $y = 0$  between  $\mu_\ell$  for  $y < 0$ , and  $\mu_r$  at  $y > 0$ . The condition for the Majorana state to form is:

$$\mu_\ell^2 < B^2 - \Delta^2, \quad \mu_r^2 > B^2 - \Delta^2 \quad (7)$$

We match the wave function at  $y = 0$ , using the ansatz  $\psi_r \propto e^{-k_r y}$  for  $y > 0$  and  $\psi_l \propto e^{k_l y}$  for  $y < 0$ . The Hamiltonian becomes:

$$\mathcal{H} = -(\Theta(y)k_r - \Theta(-y)k_l)iu\tau_z\sigma_z - \mu\tau_z + B\sigma_x + \Delta\tau_x = 0 \quad (8)$$

where  $uk_{r,l\pm} = \Delta \pm \sqrt{B^2 - \mu_{(l)r}^2}$  and the eigenvectors

$$\psi_\pm^r = e^{-(+ )k_{r(l)\pm}y} (1, e^{\pm i\theta_{r(l)}}, i, -ie^{\pm i\theta_{r(l)}})^T / 2 \quad (9)$$

with  $e^{i\theta_{r(l)}} = \mu_{r(l)}/B + i\sqrt{1 - \mu_{r(l)}^2/B^2}$ . It is straightforward to verify that  $\psi_{r(l)} \cdot \Psi = (\psi_{r(l)} \cdot \Psi)^\dagger$  are Majorana operators, with  $\psi$  a simple c-number. Thus, we find that the wave function  $\psi(y)$  of the Majorana state is

$$\begin{cases} 2i \sin \theta_r \cdot \psi_-^{(0)\ell} & y < 0 \\ (e^{-i\theta_l} - e^{-i\theta_r})\psi_+^{(0)r} + (e^{i\theta_r} - e^{-i\theta_l})\psi_-^{(0)r} & y > 0 \end{cases}, \quad (10)$$

which exhausts all possibilities for isolated majorana states.

Indeed we must note that when  $E_0$  is a spin gap, the gap  $E_1$  is due to pairing between spin-up electrons for positive  $p$  and spin-down electrons for negative  $p$ , reminiscent of a one-dimensional  $p$ -wave superconductor [10]. Recalling that vortices of a  $p$ -wave superconductor support a zero-energy bound state [2, 6, 11], we expect the formation of Majorana states when  $\Delta$  changes sign (Fig. 2e). Due to the broken azimuthal symmetry, however, two inseparable Majorana states form where  $\Delta$  vanishes.

Next we discuss *experimental realizations*. The main requirement for our proposal to be feasible is a sufficiently strong spin-orbit interaction. Spin-orbit coupling in wires adiabatically connected to reservoirs was considered long ago, both without electron-electron interactions [12] and with interactions [13] in the framework of Luttinger-liquid theory. Recently, this problem attracted renewed theoretical [14] and experimental [15] interest, both with and without external magnetic field.

Several candidate systems for quantum wires with spin-orbit interaction exist. In carbon nanotubes, spin-orbit coupling arises due to curvature effects [16]. Here it is preferable to have a strong spin-orbit coupling along the direction of propagation, requiring that the tube is bent along its axis. Alternatively, one could introduce a strong electric field perpendicular to the axis. Perhaps a more promising candidate is a wire of InAs in the wurtzite structure which is known to have strong spin-orbit coupling [17]. The velocity  $u$  in the Hamiltonian Eq. (1) is related to the experimentally measured length scale  $\lambda_{SO} = 100nm = mu$  and  $\Delta_{SO} = 250\mu V = mu^2/2$  via  $u \sim \hbar 2\Delta_{SO}\lambda_{SO} \approx 7.6 \times 10^6 cm/sec$  and  $m = \hbar^2/\lambda_{SO}^2 2\Delta = 0.015m_e$ , with  $m_e$  the free electron mass. Similar numbers (with  $\Delta = 280\mu V$ ) describe newly fabricated InSb wires, except with a large g-factor of  $\sim 50$ , compared to  $g \sim 8$  in InAs, requiring only a small, relatively innocuous to the SC, magnetic field[18].

The wire-Majorana states we envision, can be formed by spatial variations of the Zeeman field, the proximity-induced superconductivity, or, most importantly, the chemical potential, and will form near points where  $B^2 - (\mu^2 + \Delta^2) = 0$ . A varying chemical potential, as

in Fig 2d, for instance, can be achieved by gate electrodes capacitively coupled to the wire. Tunneling experiments should provide the most direct signatures of the Majorana states [19].

Additional experimental signatures can be probed by controlling the phase of the pairing  $\Delta$  in addition to the chemical potential. In particular, the configuration of Fig. 3 allows controlling the pairing phase on the left, center, and right sections independently; we denote these phases by  $\phi_\ell$ ,  $\phi_c$ ,  $\phi_r$ . The total Josephson current flowing between the three superconducting segments is rather intricate, and will be discussed in a separate publication. Since the Majoranas are localized when the distance between them,  $L$ , is infinite the Josephson current due to the Majoranas is zero. A straightforward first-order perturbation analysis for finite  $L$  yields the energy splittings between the two Majorana states on the domain walls (c.f. Ref. [20]). We find the Josephson energy associated with the Majorana fermions to be:

$$E = E_{\ell r} \cos\left(\frac{\phi_\ell - \phi_r}{2}\right) + E_c \cos\left(\frac{\phi_\ell + \phi_r}{2} - \phi_c\right). \quad (11)$$

here we assume that  $\mu_c = 0$  in the center region, and  $\mu_\ell = \mu_r = \mu$  on the sides. Also,  $E_{\ell r} \sim E_c \approx \sqrt{\frac{2\Delta B(\Delta^2 - B^2)(\Delta^2 + \mu^2 - B^2)}{\Delta^2(\Delta^2 + \mu^2 - B^2) - B\mu^2(B + \Delta)}} e^{-(B-\Delta)L/u}$ . In the similar setup of the edges of a topological insulator [21, 22] the  $E_c$ , which is a result of the tunneling from the left and the right sections to the middle section is absent since the center region between the Majoranas is not in proximity to a superconductor. We notice two prominent effects. First, by letting  $\phi_c = \phi_r$ , for instance, we see that the Josephson current from the left superconductor is  $4\pi$  periodic. More interestingly, when we try to draw current from the center region, the current, proportional to  $E_c \sin((\phi_\ell + \phi_r - 2\phi_c)/2)$  is drawn equally from the left and right superconductors. Therefore this geometry can serve as a Josephson transistor, since a change of  $\phi_R$  determines part of the current between the left and the middle section. Related effects were discussed in Ref. [23].

Next, let us estimate the Josephson tunneling strengths in the setup of Fig. 3, with three independent superconducting substrates. If the substrates are properly insulated from each other, only Josephson currents will be carried through the quantum wire via proximity; these will be given by Eq. (11), in addition to a contribution proportional to  $\Delta$  which is  $2\pi$  periodic in  $\phi_r - \phi_c$  and  $\phi_\ell - \phi_c$ . For the energy scales associated with the *InAs* wires, we expect the critical current for the  $2\pi$  periodic portion to be of order  $40nA$ , consistent with  $B, \Delta \sim 1K$ . The  $4\pi$ -periodic critical Majorana-Josephson currents,  $2eE_c/\hbar$  and  $2eE_{\ell r}/\hbar$ , are a significant fraction of this number. For instance, for *InAs* parameters with  $\mu_c = 0$  and  $\mu_r = \mu_\ell = 0.9B$  and  $\Delta = 0.8B$ , with  $B \sim 1K$ , we obtain  $E_c \approx 0.22Ke^{-L(B-\Delta)/u}$ , corresponding to a maximum current  $eE_c/\hbar \approx 4nA \cdot e^{-L/3\mu m}$  with  $L$  the



FIG. 3.  $\mu$ ,  $B$  or  $\Delta$  are tuned so that in the middle superconductor we have a spin gap while the other superconductors have a superconducting gap. In this configuration, it is possible to manipulate the two junctions separately by changing the superconducting phase difference between the neighboring regions.

separation between the Majoranas. The unique flux periodicity of the Majorana-Josephson currents can also be probed with low-frequency shot noise would also reveal the anomalous Josephson periodicity.

In this manuscript we have shown that wires with strong spin-orbit coupling in proximity to a superconductor host an interesting effective helical state. By tuning the superconducting gap  $\Delta$ , the spin gap  $B$ , or the chemical potential  $\mu$ , Majorana states can be created and detected in various experimental ways. By fabricating a set of gates over a network of such wires, we can imagine adiabatically creating Majorana pairs, moving, and even interchanging them along the network using pulse sequences in the gates. The non-Abelian character of the system should become apparent in such networks. Methods to manipulate the Majorana modes and experimental consequences for the conductance will be the subject of a future manuscript.

While finishing this manuscript we became aware of the preprint [24] which has some overlap with our results.

*Acknowledgements.*— We would like to thank Joel Moore, Jason Alicea, Erez Berg and Oleg Starykh for enlightening discussions. The research was supported by ISF, DIP and BSF grants, as well as Packard and Sloan fellowships and from the Institute for Quantum Information under NSF grants PHY-0456720 and PHY-0803371.

- 
- [1] C. Nayak *et al.*, Rev. Mod. Phys. **80**, 1083 (2008).
  - [2] G. Moore and N. Read, Nucl. Phys. B **360**, 362 (1991).
  - [3] T. M. Rice and M. Sigrist, J. Phys. C **7**, L643 (1995).
  - [4] L. Fu and C. L. Kane, Phys. Rev. Lett. **100**, 096407 (2008).
  - [5] J. Nilsson, A. R. Akhmerov, and C. W. J. Beenakker, Phys. Rev. Lett. **101**, 120403 (2008).
  - [6] J. D. Sau, R. M. Lutchyn, S. Tewari, and S. Das Sarma, Phys. Rev. Lett. **104**, 040502 (2010).
  - [7] C. Xu and J. E. Moore, Phys. Rev. B **73**, 045322 (2006).
  - [8] C. Wu, B. A. Bernevig, and S.-C. Zhang, Phys. Rev. Lett. **96**, 106401 (2006).
  - [9] J. Sun, S. Gangadharaiah, and O. A. Starykh, Phys. Rev. Lett. **98**, 126408 (2007).
  - [10] Similar to the case of topological insulators the analogy can be made precise by a unitary transformation [4].
  - [11] N. Read and D. Green, Phys. Rev. B **61**, 10267 (2000).
  - [12] A. V. Moroz and C. H. W. Barnes, Phys. Rev. B **60**,

- 14272 (1999).
- [13] A. V. Moroz, K. V. Samokhin, and C. H. W. Barnes, Phys. Rev. B **62**, 16900 (2000).
- [14] K. Hattori and H. Okamoto, Phys. Rev. B **74**, 155321 (2006).
- [15] J. Wan, M. Cahay, P. Debray, and R. Newrock, Phys. Rev. B **80**, 155440 (2009).
- [16] F. Kuemmeth, S. Ilani, D. C. Ralph, and P. L. McEuen, Nature **452**, 448 (2008).
- [17] C. Fasth *et al.*, Phys. Rev. Lett. **98**, 266801 (2007).
- [18] H. A. Nilsson *et al.*, Nano Letters **9**, 3151 (2009).
- [19] Y. E. Kraus, A. Auerbach, H. A. Fertig, and S. H. Simon, Phys. Rev. B **79**, 134515 (2009).
- [20] V. Shivamoggi, G. Refael, and J. E. Moore, ArXiv e-prints (2010).
- [21] L. Fu and C. L. Kane, Phys. Rev. Lett. **102**, 216403 (2009).
- [22] A. R. Akhmerov, J. Nilsson, and C. W. J. Beenakker, Phys. Rev. Lett. **102**, 216404 (2009).
- [23] Y. Tanaka, T. Yokoyama, and N. Nagaosa, Phys. Rev. Lett. **103**, 107002 (2009).
- [24] R. M. Lutchyn, J. D. Sau, and S. D. Sarma, arXiv:1002.4033.